ORNL/TM-2024/3722

Nested Pebble Bed Blanket (NesPeB)

Vittorio Badalassi

November 2024

ORNL/TM-2024/3722

Nuclear Energy and Fuel Cycle Division (NEFCD)

NESTED PEBBLE BED BLANKET

Vittorio Badalassi

November 2024

Prepared by
OAK RIDGE NATIONAL LABORATORY
Oak Ridge, TN 37831
managed by
UT-BATTELLE LLC
for the
US DEPARTMENT OF ENERGY
under contract DE-AC05-00OR22725

CONTENTS

CONTENTS iii

ABBREVIATIONS AND ACRONYMS iv

ABSTRACT 1

1. INTRODUCTION 2

2. TECHNICAL DESCRIPTION 3

3. DESIGN JUSTIFICATIONS 8

4. TECHNOLOGY READINESS LEVEL (TRL) ANALYSIS 13

5. ANALYSIS THROUGH SIMULATIONS 15

6. CONCLUSION 16

7. REFERENCES 16

ABBREVIATIONS AND ACRONYMS

FLiBe	molten salt made from a mixture of lithium fluoride (LiF) and beryllium fluoride (BeF_2)
FNSF	Fusion National Science Facility
HTGR	High-Temperature Gas-cooled Reactor
HTR	High-Temperature Gas-cooled (HTGR) pebble-bed Reactor (in China)
ID	Inner Diameter
MCNP	Monte Carlo N-Particle code
MHD	MagnetoHydroDynamics
NESPEB	Nested Pebble Bed Blanket
OD	Outer Diameter
ORNL	Oak Ridge National Laboratory
PVD	Physical Vapor Deposition
RAFM	Reduced Activation Ferritic-Martensitic steels
SR	Sphere Ratio
TBR	Tritium Breeding Ratio
THTR	Thorium cycle High-Temperature nuclear Reactor (in Germany)
TRL	Technology Readiness Level
TZM	Molybdenum-Titanium-Zirconium-carbon alloy
VFL	Volume Fraction of the Large Sphere

ABSTRACT

Recent advances in magnetic confinement fusion technology have attracted billions of dollars of investments in startups from venture capitals and corporations [26], resulting in the development of devices aiming to demonstrate net energy gain in a self-heated burning plasma, such as SPARC [25] (under construction) and others. However, future fusion power plants must operate in regimes that will require technologies far beyond current experience. According to a National Academies of Science, Engineering, and Medicine report [26], to have nuclear fusion power plants contributing in a timely manner to the planned reduction of atmospheric carbon dioxide, a pilot plant should be built by 2035, and it should demonstrate fusion power production and the performance of the tritium fuel system (requiring a high enough tritium breeding) by 2040. A recognized key technology gap by [26] is the fusion first wall and blanket since no current blanket concept is considered satisfactory or has been built and proven.

The first wall and blanket in magnetic fusion reactors form a vital and complex system, as it must satisfy different functions such as power extraction, tritium breeding, plasma containment, radiation shielding, and safety. The list of design requirements is even longer: high enough tritium production for fusion self-sufficiency, low material activation, decay heat and shutdown dose rates, high thermal efficiency, high-capacity factor, high magnets-divertor-vacuum vessel-first wall life, low corrosion, low cost, and intrinsically safe (requiring minimal licensing). Despite fifty-plus years of research, the first wall and blanket concepts proposed suffer from fundamental technical problems and immaturity (TRL=2-3) that jeopardize the timely delivery of a commercial fusion power plant. A fusion first-wall blanket has never been built nor tested, and a "winning", practical functioning design requires enough engineering margins (high enough tritium breeding considering the uncertainty, etc.), manufacturing simplicity, ease of continuous operation, maintenance, and low cost.

A new, groundbreaking blanket concept called "Nested Pebble Bed Blanket" (NesPeB) was developed at ORNL under the successful ARPA-E GAMOW FERMI project (patent application allowed by the USPTO). The NesPeB blanket concept addresses current blanket concepts' shortcomings and technical immaturity, paving the way for accelerated delivery of fusion power plants. NesPeB is based on nested pebbles, which are binary-sized lithium-ceramic pebbles enclosed in "Beryllide" perforated and coated spherical shells, which are also binary-sized, stacked on top of each other, forming a "bed" and cooled by Nitrogen gas also "sweeping" the Helium and Tritium generated by the neutron irradiation of Lithium; the vacuum vessel plasma facing material is Molybdenum-96 and -97 with the first wall cooled by Helium while the divertor armor is made of Tungsten. The simulations of the NesPeB blanket using Fusion Reactors Models Integrator (FERMI) are encouraging as they estimate a tritium breeding ratio (TBR) greater than 1.2 using natural Lithium, acceptable pressure drop, and excellent heat transfer properties. Furthermore, the NesPeB blanket is not limited by magneto-hydro-dynamics (MHD) effects, is designed for online refueling, relies on existing tritium extraction technologies, has a simple construction, and limits the corrosion and chemical reactivity problems.

NesPeB has the potential to be transformational and disruptive since it can solve all the main, challenging technical problems of fusion device blankets and accelerate a pilot plant delivery for 10 or more years.

1. INTRODUCTION

The structures surrounding the fusion plasma that forms a plasma chamber, i.e., the first wall, the blanket, and the divertor, serve a vital role in fusion energy systems, providing tritium fuel, radiation shielding of the vacuum vessel (VV), and magnets, efficient power extraction, plasma purification, and safety barrier. A fusion first wall-blanket has never been built nor tested, and a "winning", practical functioning design requires enough engineering margins (high enough tritium breeding considering the uncertainty, etc.), manufacturing simplicity, ease of continuous operation and maintenance, and low-cost.

The main blanket concepts proposed in the literature are (1) liquid metal cooling and/or breeding, (2) solid (ceramic) breeding gas or water-cooled, (3) molten salt cooling and breeding. In Table 1, the liquid metal (Li and PbLi), solid (ceramics), and molten salt (FLiBe) concepts and the one proposed here (Nested Pebble Bed) vs key engineering requirements are compared. Colored in green are the favorable properties of the blankets, while the drawbacks are in red. The current designs are unsatisfactory ("red" drawbacks), while NesPeB looks the best.

Among the requirements in Table 1, the most important for a fusion blanket is the TBR, which is the ratio of Tritium produced vs the Tritium burnt in the fusion reaction. The TBR should be greater than 1.15 for fusion self-sufficiency, as exposed in [15]. Tritium is bred by the interaction of the neutrons generated by the D.T. fusion reaction and the Lithium in the blanket. The neutrons are generated at 14MeV but moderate and/or scatter diffusing in the blanket, broadening the neutron energy spectrum to all the energies.

Table 1: Main fusion blanket concept specifications compared with the NesPeb blanket.

	Liquid Metal (Li)	Liquid Metal (PbLi)	Solid (Ceramics)	Molten Salt (FLiBe)	NesPeB
TBR > 1.15	No ^{6}Li enrichment	^{6}Li enrichment	Be multiplier and ^{6}Li enrichment, structure minimization	Be multiplier and ^{6}Li enrichment	No ^{6}Li enrichment
Melting point	180 C	235 C	>1200 C	460 C	>1200 C
Material compatibility/ pairing	Vanadium alloy or RAFM steel, at high T requires coatings	RAFM steel or SiC - at high T requires coatings	RAFM steel and He or H_2O coolant, Best material compatibility	Corrosion and high T, no clear solution	RAFM steel, Helium and Neon coolants
Working pressure	High coolant pressure if gases are used	High coolant pressure if gases or water are used	High coolant pressure if gases or H_2O are used	Atm pressure	High coolant pressure as gases used
MHD effects	Electrical insulators required for MFE	Electrical insulators required for MFE	No MHD effects	Small MHD effects	No MHD effects
Tritium extraction	High tritium solubility/inventory, different extraction techniques needed	High tritium solubility/inventory, various extraction techniques needed	Simple & mature tritium extraction	No mature tritium extraction technology	Simple & mature tritium extraction
Safety	Very high chemical reactivity with H_2O and air	Lower chemical reactivity than pure Li	Reactivity with H_2O. Less severe reactivity with air.	Low reactivity with air. Generation of tritium fluoride gas	Risk of reactivity with H_2O is minimized
Breeder replacement	Fluid inlet/outlet	Fluid inlet/outlet	Replacement of the ceramic pellets. Relevant evolution under irradiation	Fluid inlet/outlet	Pebbles inlet/outlet
Neutron multiplier replacement	No need of neutron multiplier	No need of neutron multiplier	Replacement of the beryllium pellets/plates	Replacement of the beryllium plates	Pebbles inlet/outlet
TRL	2-3	2-3	2-3	2-3	2

Most of the designs [15] require a Lithium-6 enriched isotopic composition (from the natural 7.5% to 60%, for example) to reach a TBR>1.15 as Lithium-6 is a much better "breeder" than Lithium-7 (it produces Tritium at any neutron energy and with a very high "thermal" (0.025 eV) cross-section (936 barns)). The need for Lithium-6 enrichment, though, is a "deal-breaker", as Li-6 enrichment is expensive and has national security implications. A pure liquid lithium-cooled and bred blanket may not need Lithium-6 enrichment, but it has very high chemical reactivity with water and air and the need for electrical insulators, especially in the high magnetic fields typical of compact fusion machines.

2. TECHNICAL DESCRIPTION

A nested pebble bed blanket has high thermal efficiency, a high tritium breeding ratio (higher than 1.2) using natural lithium isotopic composition, it contains the plasma chamber, and it shields the structural containment and the magnets of fusion reactors. The nested pebble bed blanket uses reduced activation steel structures (RAFM), minimizing the production of long-term radioactive isotopes, has effectively no corrosion and reactivity problems, can sustain very high temperatures (up to 1200 °C), and can be easily refueled online without disrupting the operation of fusion reactors. Nested pebble bed blankets generate no magnetohydrodynamics phenomena, facilitate mature tritium extractions, and eliminate exposure to water moisture. The nested pebble bed blanket is regenerative, adaptable, and cost-effective.

A key parameter for all the blankets in fusion devices is the Tritium Breeding Ratio (TBR); to have a self-sustaining fusion process, a tritium breeding ratio, which is the ratio of Tritium generated by a fusion reaction versus the Tritium burnt in that reaction, should be greater than about 1.15 (see [15]). To achieve this number, fusion reactor designs require expensive, up to 90% enriched lithium-6 breeders. Using a cheap, natural lithium isotopic composition, the nested pebble bed blanket has a tritium breeding ratio greater than 1.2. Fig. 1 shows a nested pebble 100, which is comprised of solid breeder spheres 102 (a Lithium ceramic) encased within a neutron multiplier shell 104 made of beryllide (beryllium-vanadium or beryllium-titanium) compound. The breeder spheres 102 are generated through chemical and thermal processes, creating Lithium ceramic breeder spheres 102 that maximize the lithium content and tritium breeding, that are hard (e.g., they resist scratching, abrasion, and penetrations, for example) and that are resistant to high temperatures (up to 1200 °C). The breeder spheres 102 comprise compositions of lithium ceramics such as lithium oxide ($Li2O$), lithium orthosilicate ($Li4SiO4$), and/or lithium metatitanate ($Li2TiO3$). In use, a fluid such as an inert gas Nitrogen (N), for example, impinges the neutron multiplier shell 104, with some fluid flowing about its outer surface and other portions flowing through the neutron multiplier shell 104 via the perforations 106. A plurality of flow coolant distributor elements 110 are disposed on continuous portions of the inner surfaces of the neutron multiplier shell 104 and are fastened in line with the perforations 106. The fluid cools the shell 104 and the breeder spheres 102 and sweeps Helium (He), Tritium (or T), and tritiated water (HTO) (produced by the neutron-lithium nuclear reaction in the breeder spheres 102) from and through the voids 114 between the breeder spheres 102. The swept Helium, Tritium, tritiated water, and coolant inert gas flow out of the neutron multiplier shell 104 through some perforations (holes) 106 and a flow distributor 110 that has perforations 112. To maximize lithium (Li) content, the lithium ceramic breeder spheres 102 and beryllide neutron multiplier shells 104, for example, are binary-sized and have different-sized diameters, such as three-to-one diameter ratios (3:1), as do the neutron multiplier shells 104. Fig. 1 also shows a hatch 105 of the shell 104 to load/unload the spheres 102 (see also the gap 108). The hatch 105 can be mechanically coupled to the neutron multiplier shells 104 making it movable and lockable or it may be securely fastened to the neutron multiplier shells 104 with a fastener such as through a screwing or thermal bonding.

Fig. 2 shows a mockup of the nested pebble (gold color) that has a series of perforations (holes) 106, rendering it a porous pebble. The shell is filled with lithium ceramic pebbles (in white). The flow coolant distributor elements 110 have a plurality of inward perforations (holes) 112 smaller than the outer surfaces perforations 106 of the neutron multiplier shell 104 and smaller than the breeder spheres 102 to keep the flow section comparable to the section 106 but restricting the exhaust of the breeder spheres 102.

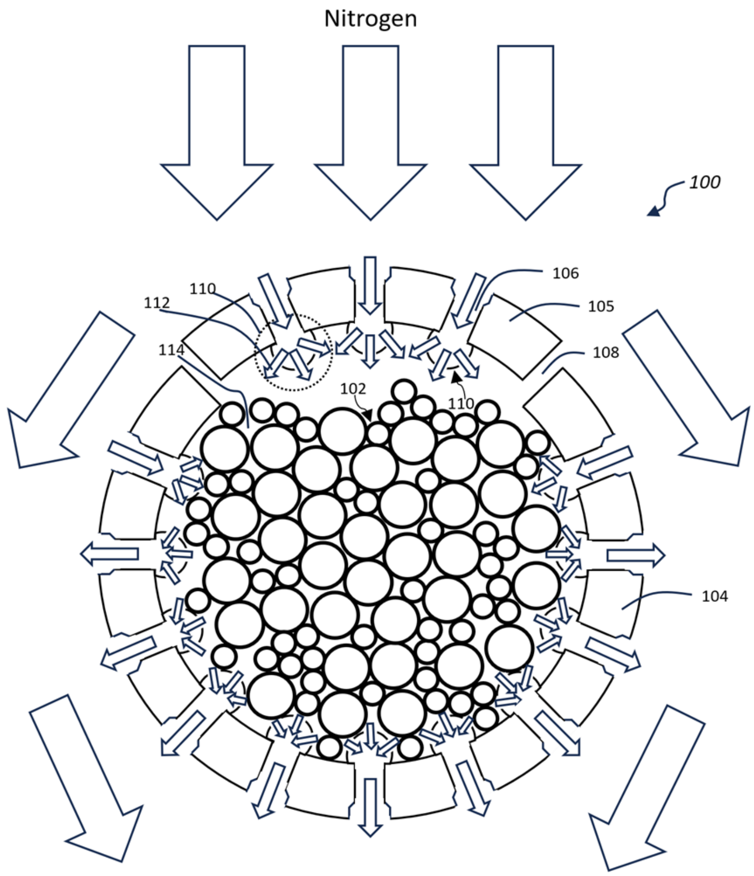

FIG. 1: an enlarged cross-sectional view of the "nested pebble" composed of tritium breeding spheres (e.g., lithium ceramics) enclosed within a neutron multiplier shell (e.g., beryllide) showing coolant flow (e.g., neon) through the neutron multiplier shell, purging various gases (Tritium, Helium, tritiated water steam, and minor others).

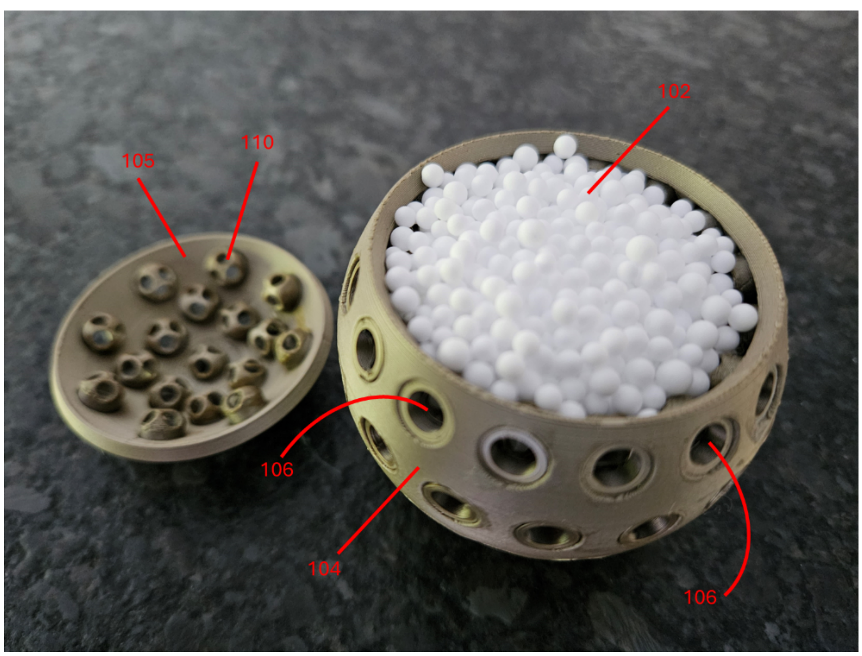

FIG. 2: a mockup of the nested pebble (gold color) filled with Lithium ceramic pebbles (in white).

Fig. 3 shows a fusion reactor 402 that has a donut-shaped toroidal vacuum chamber 406 containing the plasma 408. Fusion nuclear reactions happen in the plasma, which is confined within the donut-shaped vacuum area by magnetic fields generated by electric currents that flow through the coils.
The magnetic confinement prevents the fusion plasma from coming into contact with the inner first wall 502 that surrounds the donut-shaped toroidal vacuum chamber 406, preventing the fusion plasma from disrupting the fusion process and melting the first wall 502. A packing and/or an array of a plurality of nested pebbles 100 positioned directly adjacent to each other comprise the nested pebble bed blanket 403 that surrounds a vacuum chamber 406 of the fusion reactor 402. The nested pebble bed blanket 403 is exposed to a neutron flux generated by the fusion plasma 408. In the fusion reactor 402, the neutrons are multiplicated by the neutron multiplier shells 104, such as by beryllide (beryllium-vanadium and/or beryllium-titanium compounds) shells, and interact with the breeder spheres 102 (e.g., lithium ceramic spheres), heating the nested pebble bed blanket and generating helium (He), tritium (H or T), tritiated water (HTO), and in minor quantities, lithium hydroxide LiOH and other elements that diffuse out of the spheres into the coolant/sweeping gas (Nitrogen). The tritiated water (HTO) is in the steam phase, and it is generated by the dissociation of oxygen that recombines with Tritium generated by the neutron reactions with the Lithium in the ceramic breeder spheres 102. An inert gas such as Nitrogen is pumped by a blower 603 from a top area 5 of reactor 402 and flows downward. It cools the nested pebble bed blanket 403, which is heated by the volumetric heat generated by the neutrons released from the fusion plasma 408 interacting with the nested pebbles 100 in the blanket, and it collects/sweeps the gases generated by the neutrons- breeder spheres 102 reactions, i.e., Helium, Tritium, tritiated water and small quantities of other gases. The Nitrogen rich new gases flows through the holes in the perforated hoppers 401, and are collected near the bottom of reactor 402. The replenishment system enables automatic nested pebble bed blanket rejuvenation through an automatic replenishment system and transfer process managed by a processor and/or controller. The nested pebbles 100 are loaded from the top of reactor 402 by a replenishment system such as an automated conveyor system 412. Spent embedded neutron multiplier shells 104 are exhausted through the hoppers 401. The holes of the perforated hoppers 401 are configured and calibrated to allow Nitrogen to pass through to a gas loop while guiding the nested pebbles 100 down to a transfer conveyor system 414 near the bottom of reactor 402. The nested pebble bed blanket 403 is contained and separated from the vacuum chamber by a first wall composed of a sandwich of materials such as a plasma- facing refractory material 502 and a steel material 504 cooled by an inert gas such as helium 506 and a structural ring 400. The steel wall portion 504 is adjacent to an inert gas channel 506.

Fig. 4 shows in detail the first wall that surrounds vacuum area 406 as a first barrier to the hot plasma and contains the nested pebble bed blanket. The first wall is a sandwich of materials, e.g., a plasma-facing refractory material 502 and a steel 504, which is cooled by an inert gas such as Helium flowing in cooling channels 506. The refractory material wall can be made of Tungsten or it can comprise titanium (Ti), zirconium (Zr), and one or two isotopes of molybdenum (e.g., 96Mo and/or 97Mo), for example. More specifically, the refractory material wall 502 comprises titanium zirconium-molybdenum (TZM) alloy containing a 0.5% titanium element, a 0.08% zirconium element, a 0.02% carbon element, and 99.4% molybdenum isotopes 96Mo and/or 97Mo to limit long term radioactive waste. The refractory material wall 502 is adjacent to a steel 504 that conveys thermal energy induced by the fusion plasma to a coolant flow channel 506 that removes that thermal energy. Helium is pumped by the blower 601 from the bottom area of reactor 402 and flows upward in channel 506, cooling the fusion-facing wall 502. It is collected near the top of the reactor 402.

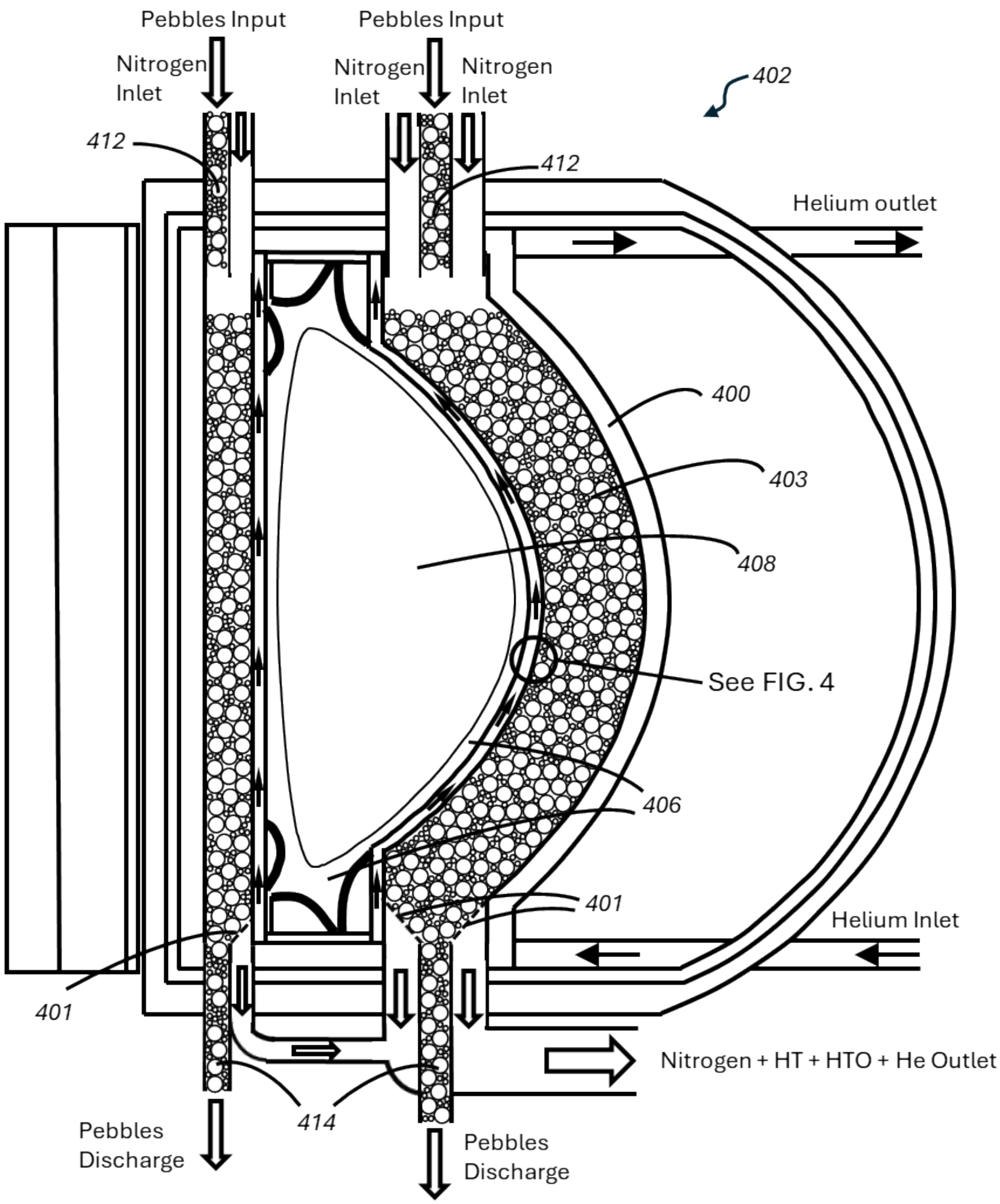

Fig.3: cross-sectional schematic of a fusion reactor with a nested pebble bed blanket swept by a coolant inert gas (e.g., neon) and rejuvenated by a replenishment system.

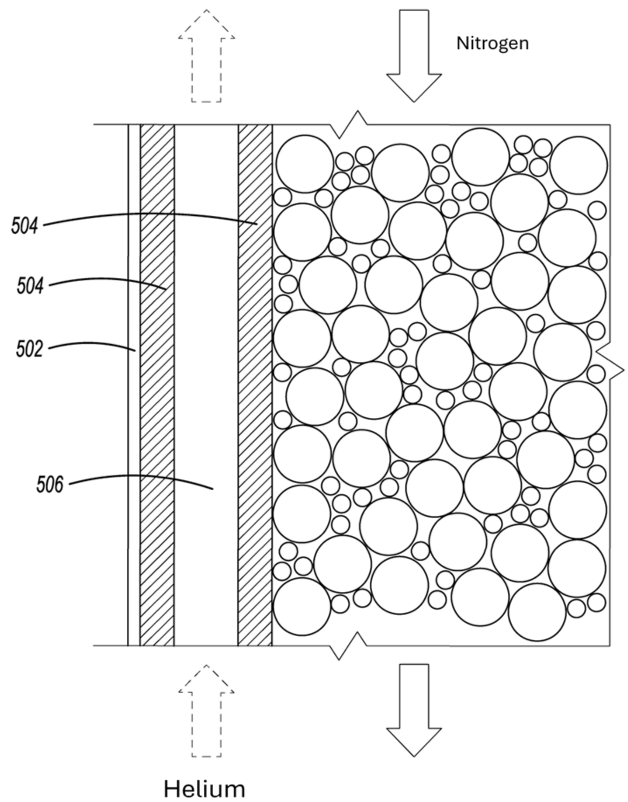

Fig. 4: enlarged cross-sectional view of the plasma-facing refractory "first wall", its cooling channel, and part of the blanket.

Fig. 5 shows a thermal-hydraulic system for the fusion reactor 402. In operation, Nitrogen rich of Tritium, Tritiated water steam, and Helium is discharged near the bottom of reactor 402 and flows to a first heat exchanger 602. The first heat exchanger, 602, transfers the thermal energy (heat) of Nitrogen gas to a cooler fluid such as a molten salt (e.g., molten nitrate), which heats up and is then pumped to a thermal storage system and/or a power conversion process or a power generating cycle to generate electricity, for example, or other power. Some power cycles use carbon dioxide (CO2) or water (steam) during the power generating cycle. Also in Fig. 5, the Lithium breeding generates important products for the fusion fuel, e.g., Tritium and tritiated water, that are extracted (along with other products and impurities such as Helium and lithium hydroxide) from the Nitrogen rich of Tritium, tritiated water steam, and helium mixture by a separator/purifier 604 and then pumped back into the blanket by the blower 603. Tritium, tritiated water, and other gas levels must exceed a predetermined concentration in pure Nitrogen before an efficient separation occurs. For example, when one percent concentration of tritiated water (HTO), tritiated hydrogen (HT), and Helium (He) with respect to the total amount of Nitrogen mass is reached, separator/purifiers 604 is able to remove most of them from Nitrogen by extraction and a purification process or system. The purified Nitrogen is recirculated back into the Nitrogen loop. A second heat exchanger, 606 transfers the thermal energy of the hot Helium that cools the reactor's first wall (composed of walls 502 and 504) to a second cooler fluid, which can again be molten salt (e.g., molten nitrite). The cooled Helium referred to as processed Helium, is then pumped by the blower 601 into reactor 402 to continue cooling the first wall 502 through the coolant channel 506, while the molten salt carries the thermal energy to a thermal storage system and/or to a power cycle that produces electricity.

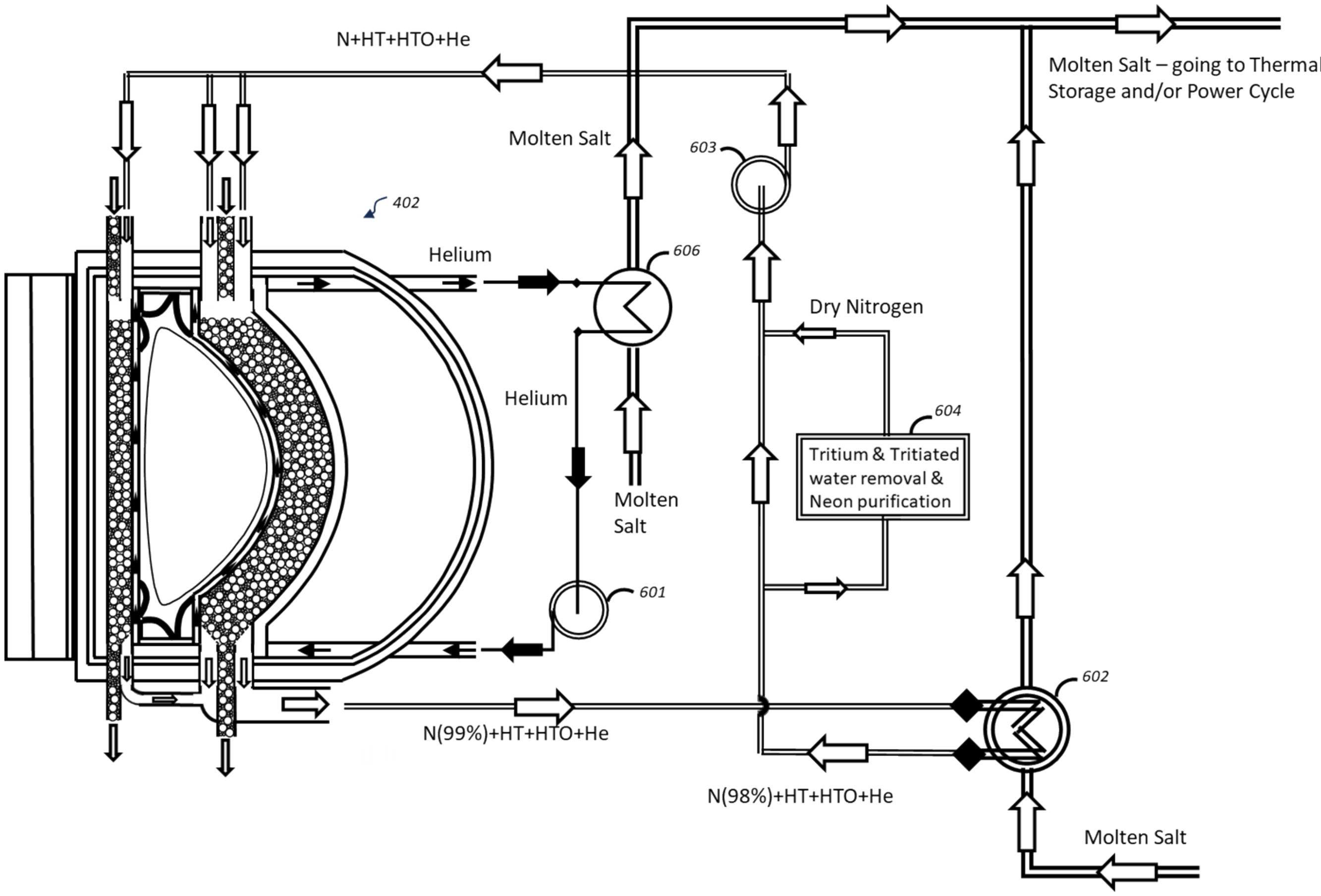

Fig. 5: enlarged cross-sectional view of the plasma-facing refractory "first wall", its cooling channel, and part of the blanket.

3. DESIGN JUSTIFICATIONS

A way to increase the tritium breeding ratio is to maximize the lithium content, making the breeder spheres 102 and the neutron multiplier shell 104 (collectively referred to as nested pebbles 100) spherical and binary-sized. A sphere size ratio (SR) of 3 and a Volume Fraction of the Large sphere (VFL) of 0.7 increases the solid random packing fraction (fraction of the total sphere volume versus available volume) from 0.64 (single size spheres) to 0.71. Higher size ratio spheres have even higher random packing fractions. For example, a sphere size ratio of 5 allows a maximum packing fraction of about 0.76 (see Fig. 6). In the use case of 3:1 diameter ratios in the binary-sized breeder spheres 102, the large spheres may have a diameter of 2.4 mm, and the small spheres may have a diameter of about 0.8 mm, respectively. The inner perforations (holes) 112 of the flow distributors 110 in the multiplier spherical shell 104 would have a diameter of less than 0.8 mm (e.g., 0.7 mm) to retain the small breeder sphere 102 within the neutron multiplier spherical shell's 104 inner volume. The perforations (holes) 106 (that lead the flow to the flow distributors 110) of the neutron multiplier shell 104 may have a diameter of less than 2.4 mm, which retain the large breeder spheres 102 in the multiplier shells 104 in case of a rupture of a flow distributor 110. In the case of 3:1 diameter ratios in the binary-sized multiplier spherical shells 104, the large spherical shell may have a diameter of about 6 cm, and the small one has a diameter of about 2 cm. When the volume fraction of large breeding spheres and multiplier spherical shells (VFL) is 0.7, and the size ratio (SR) is 3, there are eleven times the small breeder spheres 102 and small neutron multiplier spherical shells 104, respectively, than the large breeder spheres 102 and the large neutron multiplier spherical shells 104, respectively. Further, the spherical shape of the beryllium (beryllide) neutron multiplier shells 104 encasing lithium breeder spheres 102 facilitate neutron backscattering inside the shell. Alternative single-size shapes of spheres 102 and shells 104, such as ellipsoids with axes ratios near 1.25:1:0.8 or other shapes, can be envisaged so that the packing fraction (of lithium ceramics spheres 102 and/or nested pebbles) is still higher than 0.6 and avoiding the use of flow distributors.

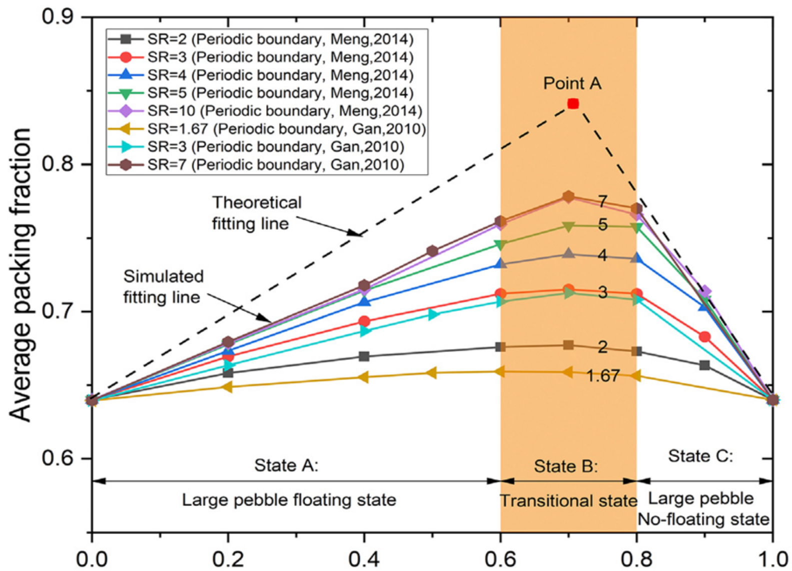

Fig 6: Average packing fraction vs Volume Fraction of Large Pebble (VFL) for binary-sized pebbles randomly arranged [1].

Further, when the binary-sized breeder spheres 102 comprise lithium oxide (Li2O) and the neutron multiplier binary-sized spherical shells 104 comprise a beryllide compound with a shell thickness of about 1 mm, the nested pebble bed blanket's 403 overall lithium content is about 0.42 g/cm3, which is greater than prior art molten salt blankets, comprising a mixture lithium fluoride (LiF) and beryllium fluoride (BeF2) called FLiBe, of about .27 g/cm3. Further, Lithium oxide (Li2O) has higher lithium atom density compared to other lithium compositions (0.93 g/cm3 vs 0.54 g/cm3 in lithium orthosilicate Li4SiO4, for example); notably, the overall lithium content of the nested pebble bed blanket 403 approaches pure liquid lithium blankets of 0.45 g/cm3, which is lower than the pure liquid lithium density of 0.51 g/cm3 because of steel structures. However, pure liquid Lithium may not be used in large quantities due to its reactivity (flammability) with air, moisture, and water, corrosiveness with steels, and chemical toxicity.

Nested pebbles 100 made of binary-sized (3:1 ratio) lithium oxide (Li2O) breeder spheres 102 included in beryllide compound neutron multiplier spherical shells 104 achieve a tritium breeding ratio exceeding 1.2. This tritium breeding ratio is realized using a natural lithium composition in the breeder spheres 102, i.e., 7.5% Lithium-6 and 92.5% Lithium-7. This is in contrast to conventional reactor blankets that use up to about 90% enrichment in Lithium-6 to attain a comparable tritium breeding ratio. Lithium oxide (Li2O) also has a strong thermal conductivity (3 W/(mK)), and the breeder spheres 102 made of lithium oxide (Li2O) function at a high-temperature operational range (400 °C – 600 °C).

The use of a fast-sweeping Nitrogen coolant that comprises no helium content enables more efficient extraction of the Helium produced by fusion reactions because of its speed and absence of limiting diffusion resistance in comparison to using a low-speed helium sweeping gas (as used in current fusion reactor solid blankets design), reducing the lithium oxide breeder sphere 102 swelling and so preserving their integrity. Additionally, Nitrogen is unreactive with Lithium oxide at high temperatures, and it is cheap. Neon could also be used because of its superior thermal properties since it has high thermal conductivity, heat capacity, and low viscosity, but it is expensive, while Argon (another option) activates under irradiation.

Production of the corrosive lithium hydroxide (LiOH(T)) is kept at low levels by the fusion reactor's separator/purifier 604, where lithium hydroxide (LiOH(T)) is extracted (along with tritiated hydrogen (HT), helium (He), and tritiated water (HTO)). Further, the beryllide neutron multiplier shells 104 resist oxidation, making it resistant to the lithium hydroxide (LiOH(T)) induced corrosion.

In the use case, beryllium (beryllide compound Be-V and/or Be-Ti) is used in the neutron multiplier shells 104 because of its low energy threshold (e.g., 1.86 MeV) for (n,2n) neutron multiplication. A (n,2n) reaction represents a neutron-induced reaction when a neutron collides with a target nucleus, ejecting the two neutrons. Further, beryllium has a very low neutron absorption, has a high melting point (1287 °C), is lightweight, resists indentation, scratching, and abrasion (e.g., it is stiff), is a good thermal conductor, is non-magnetic. Beryllide compounds share all the beryllium properties, but in contrast to pure beryllium, they have the added advantage of not deforming meaningfully because of their desorption properties of helium and tritium gases generated by neutron irradiation. Comparatively, beryllide has a density thirty percent lower than aluminum and a stiffness three times greater than titanium. As a consequence, the nested pebbles 100 can be made of very light materials, e.g., beryllide (Be-V and/or Be-Ti) and a lithium ceramic (Li2O), resulting in a small gravity load in the blanket's nested pebble staking and the disclosed beryllide neutron multiplier shells 104 do not need steel structures to maintain their structural integrity, maximizing the nested pebble bed blanket's tritium breeding ratio; further the thinner are the shells (e.g., ST = (outer diameter (OD) – inner diameter(ID))/2) the higher is the tritium breeding ratio.

The stacking and the geometry of nested pebbles 100 facilitate automatic and continuous replacement that may be based on a reactor's tritium breeding efficiency. When a surface coating material, such as titanium nitride (TiN), is applied to the nested pebbles, the coefficient of friction among the nested pebbles is reduced from 0.5 (beryllium-beryllium) to 0.11 (titanium nitride-titanium nitride), facilitating the nested pebble's movements during the recharging and unloading. Further, such coating eliminates the health risks associated with beryllium (beryllide) powder generated from the nested pebbles "rubbing" with each other in their movements, including the potential for respiratory illness and skin disease.

In the fusion reactor 402 shown in the cross-section in Fig. 4, typically one-third of the heat produced by the fusion reaction may be transferred to the first-wall 502 (by plasma irradiation and charged particles - surface heating) while two-thirds of the heat may be transferred to the blanket, i.e., the nested pebble bed blanket heated by volumetric heating induced by the neutron flux-pebbles interaction. The fusion reactor's helium coolant dissipates heat from the first wall efficiently through its heat transfer properties (high thermal conductivity, high heat capacity, and low viscosity), and its ability to operate at high temperatures without becoming reactive with any material; the refractory material 502 that serves as the plasma-facing wall 502 comprises titanium (Ti), zirconium (Zr), or TZM because of its outstanding physical properties comparable to Tungsten. Molybdenum, though, has a much lower atomic mass, generating substantially higher radiative power losses. The -96 and -97 isotopes of molybdenum (e.g., 96Mo and/or 97Mo) are chosen to avoid long-term radioactive waste, as proven in [5] (see Fig. 9). Further, Molybdenum is quite stable under neutron irradiation (low transmutation rate) and can actually multiply neutrons above 7 MeV (see (n,2n) in Fig. 8). Tungsten has been used typically for first-wall and divertor armor, and a comparison of the two is shown in Table 2.

The titanium-zirconium-molybdenum alloy comprises a molybdenum alloy containing 0.5% titanium, 0.08% zirconium, and 0.02% carbon with the balance (99.4%) molybdenum -96 and -97. The alloy reduces the likelihood that the plasma facing wall 502 becomes brittle at high temperatures (TZM has a higher recrystallization temperature than pure molybdenum). Moreover, titanium-zirconium-molybdenum behaves much like Tungsten, with up to fifty displacements per atom and with high strength, hardness, creep resistance, and ductility, and without any disadvantages of Tungsten, as shown in Fig.7.

TZM further has a higher recrystallization temperature than pure molybdenum, reducing the likelihood of embrittlement at higher temperatures and in elevated temperature applications, TZM's higher strength, hardness, creep resistance, and ductility ensure it will not weaken or soften. Further, with neutron damages up to 50 dpa, TZM behaves very closely to Tungsten (Fig. 7, [29]). Because of the points above TZM with Molybdenum in its isotopic composition -96 and -97 is preferred to Tungsten here as a first wall material.

Table 2: Tungsten vs. Molybdenum

Property	Tungsten (W)	TZM (Ti-Zr-^{96}Mo-^{97}Mo)
Melting point	3422 °C	2623 °C
	Tungsten is more resistant to the extremely high temperatures found in fusion reactors.	
Thermal conductivity	170 W/mK	118 W/mK
	Tungsten transfers heat more effectively than molybdenum from plasma-facing surfaces.	
Sputtering Yield	Similar	
Hydrogen retention	W lower than TZM TZM's higher hydrogen retention may degrade plasma performance more than tungsten.	
Long-term neutron activation	W has a lower long-term activation than TZM but when TZM is enriched with isotopes -96 and -97, its long-lived radioisotopes are dramatically reduced.	
Mechanical properties	W is more brittle than TZM. Flexibility (less brittle) is preferred to accommodate thermal and mechanical stresses.	
Density	19.25 g/cm^3	10.16 g/cm^3
	TZM is much lighter than tungsten; this helps structurally.	
Atomic (Z) number	74	42
	Tungsten has a much higher atomic number than TZM, with the chance of generating substantially higher radiative power losses.	

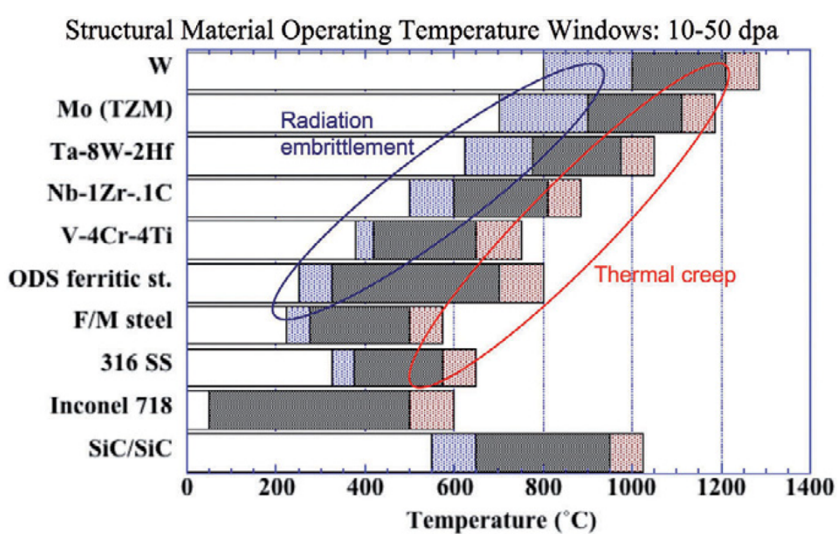

Fig 7: Estimated operating temperature windows (dark shaded region) for structural materials in nuclear energy systems for damage levels of 10 to 50 dpa. The light blue and red regions represent lower and upper temperature uncertainty bands [29].

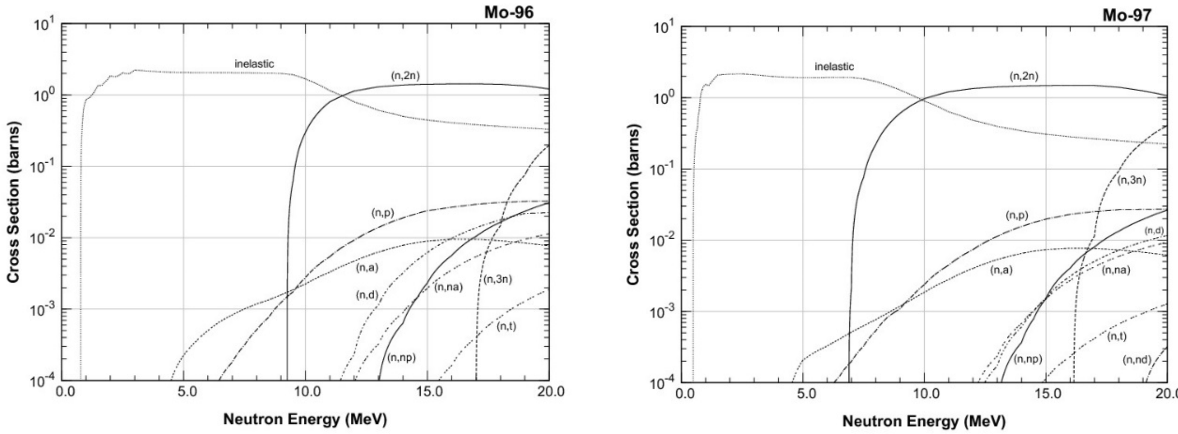

Fig. 8: neutron cross sections of Molybdenum-96 and -97.

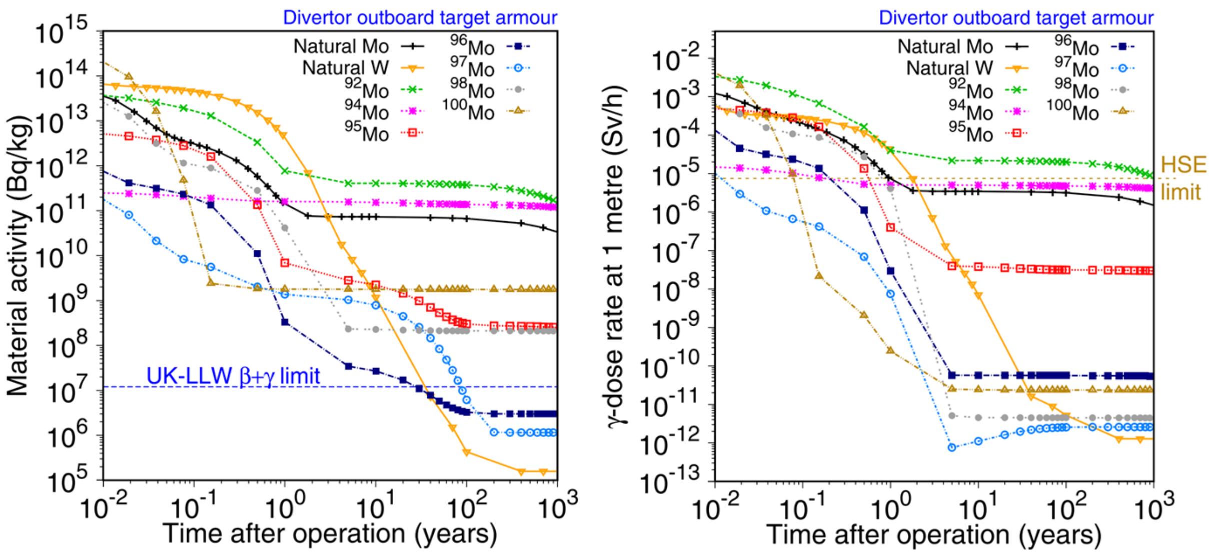

Fig. 9: Simulation results Mo isotopes after a 5-year exposure to the divertor armor spectra (ITER). From Gilbert et al. [5].

The molten salt in Fig. 5 may comprise a molten nitrate salt combination by mass of 43% potassium nitrate (KNO3), 40% sodium nitrate (NaNO2), and 7% sodium nitrate (NaNO3) that possesses a low melting point (142 °C), a high boiling point (593 °C), it is not corrosive, exhibits insensitivity to radiation damage, does not undergo reactions with lithium oxide (Li2O), has high thermal conductivity, and is liquid at atmospheric pressure. This type of molten salt (e.g., molten nitrates) is preferable for thermal storage applications or as an intermediate fluid to insulate neon from water. In systems that adjust electricity generation to match changes in demand for power (e.g., load-follow generation), thermal storage allows an easy change of electric output from the fusion power plant. Further, thermal storage provides the thermal inertia needed to balance the discontinuous power production in typical fusion reactors. The heat transfer salt is maintained at atmospheric pressure (0.1 MPa), while the neon and helium coolants are pressurized at 8 Mpa. Thus, should a heat exchange element rupture (e.g., a tube shell), the neon and Helium circulating in the fusion reactor will discharge into the molten salt, impeding their contamination with the molten salt.

4. TECHNOLOGY READINESS LEVEL (TRL) ANALYSIS

The supporting technologies of NesPeB - single components like lithium oxide pebbles or systems such as purification plants, etc. - can be acquired from other technical fields. For example, the pebble bed concept was validated in fission reactors as well as pebble conveyors and hoppers (Figure 10(a,b)).
Beryllium shells, similar to the nested pebbles, were built for aerospace gyroscopes (Figure 11(a) top); precise laser drilling can be used for the Beryllide shells perforations, physical vapor deposition (PVD) for the Titanium Nitride coating on the Beryllide shells (used before in coated drills, see fig. 11 (a) bottom). Further, Li_2O pebbles have been manufactured by wet process (Figure 11(a) middle, see [6,7]).
The purification plant to separate Tritium, tritiated water, and other impurities from Nitrogen is almost identical to HTGR fission reactors (THTR-300 in Germany and HTR-300 in China [33], i.e., with TRL=9). The picture in Figure 11(b) represents the purification and extraction plant of THTR-300 (300MW) that ran in the 1980s for several years and is similar to the currently running Chinese HTR-PM. The gases separated from Helium by the THTR are Hydrogen and Water. Carbon monoxide & dioxide, Oxygen, Nitrogen, and incondensable heavy fission gases are also extracted but do not apply to the NesPeB. There is also a dust filter that, in our case, can remove the lithium hydroxide. The THTR 300 MW purification plant could separate up to 76g/day of hydrogen, almost the same as 75g/day of Tritium for a fusion reactor of the same power [33].
Table 3 gives the particular TRL levels of the various components of the NesPeB blanket. While most of the components of NesPeB have a TRL level of at least 6, the overall TRL level cannot be greater than 2 (concept created and verified by simulations) because there is no hardware yet built to test the concept. The path to higher TRL levels, though, is quite straightforward as a simple irradiation experiment of a subset of the pebble bed would be enough to boost the overall TRL to 5-6.

(a)

(b)

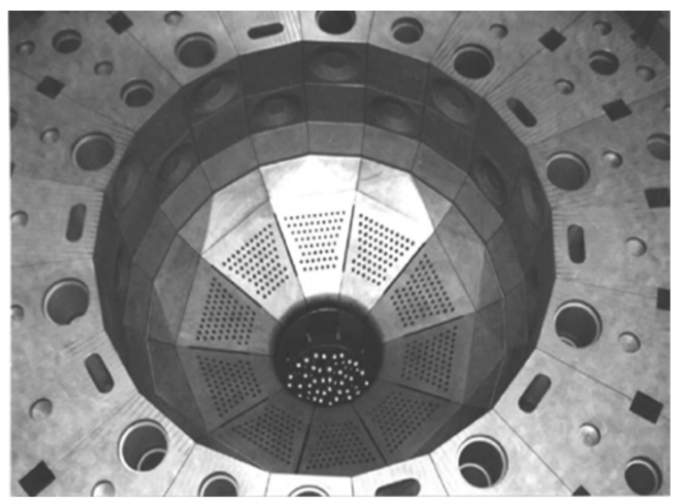

Figure 10: (a) the core of the Pebble Bed fission reactor THTR-300 (Germany) (b) the hopper of the Pebble Bed fission reactor HTR-300 (China)

(a) (b)

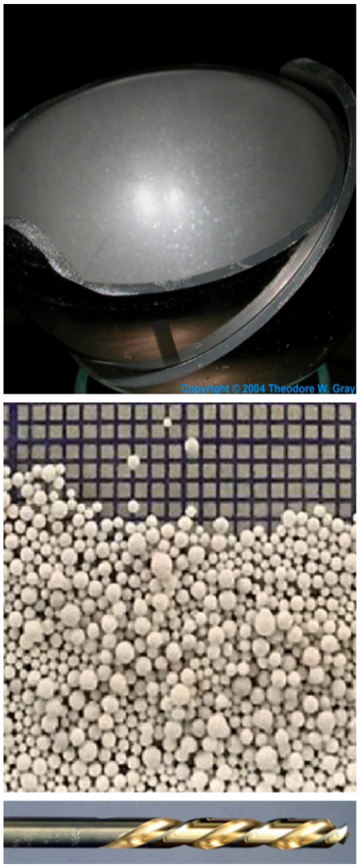

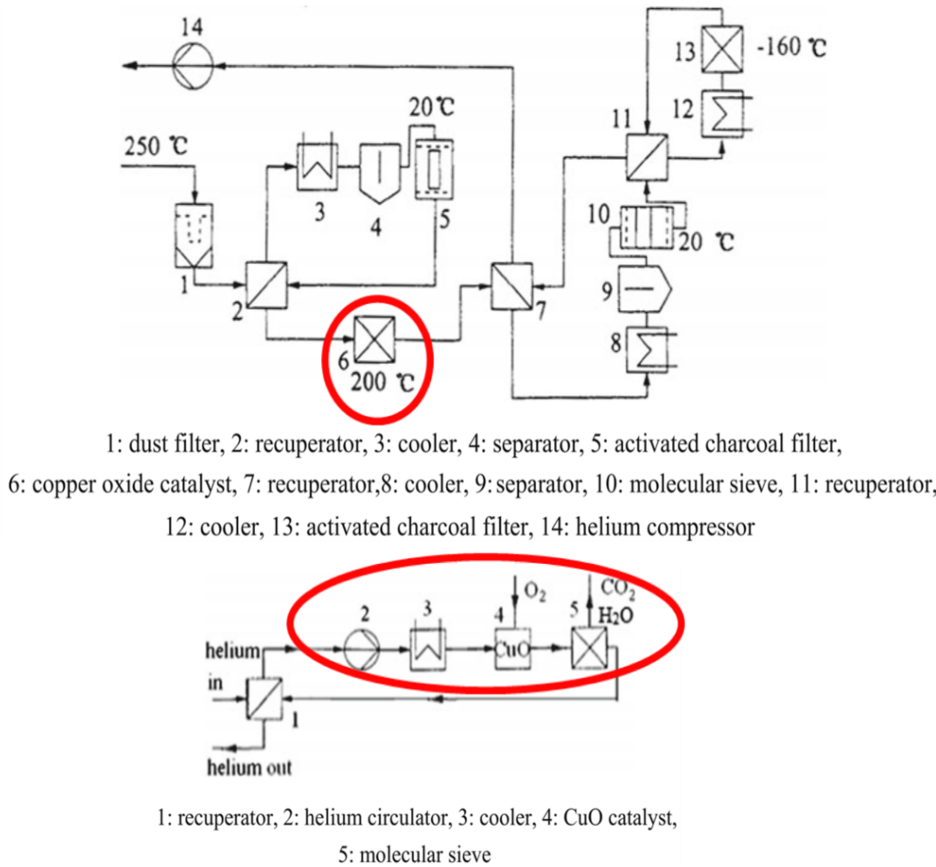

Figure 11: NesPeB already proven technologies: (a) top Beryllium spherical shell from gyroscopes (1.5-inch diameter), (a) middle, Lithium Oxide Pebbles [6,7], (a) bottom, Titanium Nitride coated drill, (b) Scheme of the THTR gas purification plant [33].

Table 3: NesPeB Technology Readiness Level and Manufacturing Readiness Level analysis

TRL	1	2	3	4	5	6	7	8	9
Nested Pebble									
Nested Pebble bed concept									
Pebble bed concept									
Pebbles conveyors									
Fuel Cycle									
Thermodynamic cycle									
Tritium extraction									

MRL	1	2	3	4	5	6	7	8	9	10
Beryllium shell										
Lithium oxide pebbles										
Titanium Nitride Coating										
Tungsten plasma facing material										

5. ANALYSIS THROUGH SIMULATIONS

The first simulations of the NesPeB blanket using MCNP (Monte Carlo N-Particle code [40]), part of the Fusion Reactors Models Integrator (FERMI) [2] software suite, are encouraging as they estimate a tritium breeding ratio (TBR) greater than 1.2 using natural Lithium for a typical "Fusion National Science Facility" (FNSF) [39]. The pressure drop across the blanket calculated with the OpenFoam-FERMI code [2] and approximating the Nested Pebbles with a porous media following validated procedures used in fission pebble bed reactors [42] was found to be 4.65% of the total pressure (8MPa). Such value is less than 5% of the total, and it is considered an acceptable loss from an engineering point of view.
Further, the nested pebble simulations demonstrated excellent heat transfer properties. Single pebble simulations were conducted with representative flows up to 1 m/s fluid velocities (Fig.11(a),(b)), and the Li2O pebbles never got close to the melting point temperature (1438C).
The current results are summarized in Table 4; a full blanket parametric study and optimization using simulations are ongoing, and the results will be used to verify the concept. Experimental results will be needed for a complete validation.

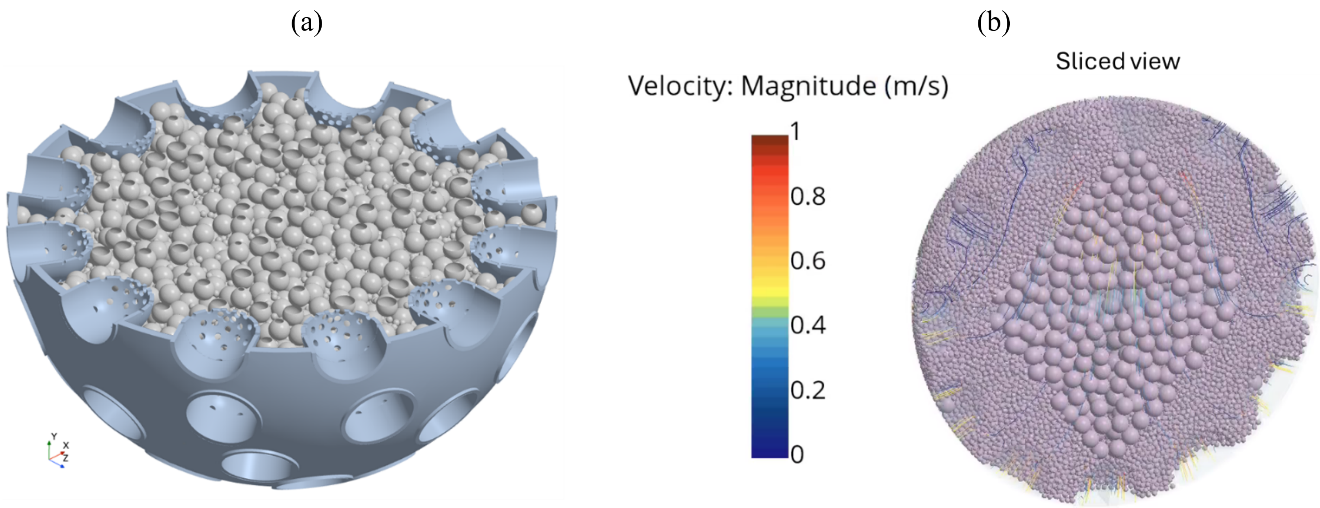

Figure 12: (a) detail of the Nested Pebble CAD, (b) detailed simulation with a 1m/s impinging velocity.

A separate TM report with the details of the simulations and models is being prepared.

Table 4: Performance metric for the NesPeB blanket that will be evaluated with experiments and simulations

	Metric	Project Goal	Design Outcome	FERMI
1	NesPeB Tritium Breeding Ratio with natural Lithium isotopic composition	1.2	Fusion self sufficiency	1.21
2	Blanket pressure drop	< 5% of the total inlet pressure	Power efficiency	4.68%
3	Optimal Temperature range for breeding pebbles and shells	350-700C for Li2O 350-550 for the Beryllium shells	Optimal, reliable tritium production Acceptable Beryllium shell deformation	√
4	Lithium hydroxide (LiOH) concentration	< 70 ppm	Low corrosion	TBD
5	Stability and integrity of the shells coating (Titanium Nitride)	Coating does not peel off nor degrades meaningfully under irradiation	Nested Pebbles can move against each other	TBD
6	Integrity of the breeding pebbles (Lithium Oxide)	Acceptable swelling, no failures	Reliable tritium production	TBD
7	Integrity of the Beryllium (Aluminum) shell	No failures allowed	Integrity of the Nested Pebble Bed	TBD

6. CONCLUSION

The nested pebble bed blanket has high thermal efficiency, sustains Tritium breeding ratios greater than 1.2 using a natural Lithium isotopic composition, has moderate pressure drop, and is cooled and swept from Tritium efficiently by inert and not corrosive gases (Helium, Nitrogen) with a maximum temperature of 550 °C. The nested pebble bed blanket is unaffected by disruptive magnetohydrodynamics effects because the blanket does not rely on liquid metal coolants and/or breeders. Because the Lithium ceramic pebbles are kept insulated from water, the system prevents unintended lithium-water reactions that may create fire hazards and/or degrade the tritium breeding. The nested pebbles made of Lithium ceramic breeder spheres and neutron multiplier Beryllide shells are loaded in the blanket cavity and exhausted by continuous replenishment, i.e., the loading and unloading process and system.

NesPeB has the potential to be transformational and disruptive since it can solve all the main, challenging technical problems of fusion device blankets and accelerate a pilot plant delivery for 10 or more years.

7. REFERENCES

[1] Yongjin Feng, Baoping Gong, Hao Cheng, Long Wang, XiaoyuWang, "Effects of fixed wall and pebble size ratio on packing properties and contact force distribution in binary-sized pebble mixed beds at the maximum packing efficiency state", Powder Technology 390 (2021) 504–520.

[2] V. Badalassi, A. Sircar, J. M. Solberg, J. W. Bae, K. Borowiec, P. Huang, S. Smolentsev & E. Peterson (2023) FERMI: Fusion Energy Reactor Models Integrator, Fusion Science and Technology, 79:3, 345-379, DOI: 10.1080/15361055.2022.2151818

[3] A.K. Nath, "9.06 - Laser Drilling of Metallic and Nonmetallic Substrates", Comprehensive Materials Processing, Editor(s): Saleem Hashmi, Gilmar Ferreira Batalha, Chester J. Van Tyne, Bekir Yilbas, Elsevier, 2014, Pages 115-175, ISBN 9780080965338, https://doi.org/10.1016/B978-0-08-096532-1.00904-3.

[4] Jae-Hwan Kim, Taehyun Hwang, Suguru Nakano, Mitsutaka Miyamoto, Hirotomo Iwakiri, Masaru Nakamichi, "Deuterium desorption and retention of Beryllium intermetallic compounds for fusion applications", Journal of Nuclear Materials, Volume 550, 2021, 152936, ISSN 0022-3115, https://doi.org/10.1016/j.jnucmat.2021.152936.

[5] M.R. Gilbert, L.W. Packer and T. Stainer, "Experimental validation of inventory simulations on molybdenum and its isotopes for fusion applications", Nuclear Fusion 60, 2020, 106022.

[6] Ruichong Chen, Mao Yang, Yanli Shi, Hailiang Wang, Hao Guo, Yuanyuan Zeng, Jianqi Qi, Qiwu Shi, Zhijun Liao, Tiecheng Lu, "Low-temperature fabrication of Li2O porous ceramic pebbles by two-stage support decomposition", International Journal of Hydrogen Energy, Volume 44, Issue 36, 2019, Pages 20249-20256, ISSN 0360-3199, https://doi.org/10.1016/j.ijhydene.2019.06.009.

[7] Ruichong Chen, Jianqi Qi, Qiwu Shi, Yanli Shi, Hailiang Wang, Hao Guo, Yuanyuan Zeng, Mao Yang, Zhijun Liao, Tiecheng Lu, "Highly efficient preparation of Li2O breeder materials with core-shell structure by oil-based granulation route", Journal of the American Ceramic Society, Volume 103, Issue 10, Pages 5612-5623, 2020, https://doi.org/10.1111/jace.17336

[8] H. Kwast, et al., EXOTIC: Development of Ceramic Tritium Breeding Materials for Fusion Reactor Blankets. The Behavior of Tritium in: Lithium aluminate, Lithium oxide, Lithium Silicates, Lithium zirconates ECN-C-95-123, (1995).

[9] Guangming Zhou, Francisco Hernández, Lorenzo V. Boccaccini, Hongli Chen, Minyou Ye, "Preliminary structural analysis of the new HCPB blanket for EU DEMO reactor", International Journal of Hydrogen Energy, Volume 41, Issue 17, 2016, Pages 7053-7058, ISSN 0360-3199, https://doi.org/10.1016/j.ijhydene.2016.01.064.

[10] E. Proust, L. Anzidei, M. Dalle Donne, U. Fischer, T. Kuroda, "Solid breeder blanket design and tritium breeding", Fusion Engineering and Design, Volume 16, 1991, Pages 73-84, ISSN 0920-3796, https://doi.org/10.1016/0920-3796(91)90184-R.
[11] Kunihiko Tsuchiya, Katsuhiro Fuchinoue, Shigeru Saito, Kazutoshi Watarumi, Takemi Furuya, Hiroshi Kawamura, "Fabrication development of Li2O pebbles by wet process",Journal of Nuclear Materials, Volume 253, Issues 1–3, 1998, Pages 196-202, ISSN 0022-3115, https://doi.org/10.1016/S0022-3115(97)00312-7.
[12] D.P. Jackson et al., "A Review of Fusion Breeder Blanket Technology. Part I: Review and Findings", December 1984. Report No. CFFTP-G-84033. X-Ref Report: AECL-8631.
[13] H. Kwast, et al., "Fabrication, properties and tritium release rates of lithium zirconates", 3rd International Symposium on the Fabrication and Properties of Lithium, Ceramics, during the 93rd Annual Meeting of the American Ceramic Society (1991).
[14] Timur Kulsartov, Zhanna Zaurbekova, Regina Knitter, Asset Shaimerdenov, Yevgen Chikhray, Saulet Askerbekov, Assyl Akhanov, Inesh Kenzhina, Gunta Kizane, Yergazy Kenzhin, Magzhan Aitkulov, Darkhan Sairanbayev, Yuriy Gordienko, Yuriy Ponkratov, "Studies of two-phase lithium ceramics Li4SiO4-Li2TiO3 under conditions of neutron irradiation", Nuclear Materials and Energy, Volume 30, 2022, 101129, ISSN 2352-1791, https://doi.org/10.1016/j.nme.2022.101129.
[15] Abdou, M., Morley, N.B., Smolentsev, S., Ying, A., Malang, S., Rowcliffe, A., Ulrickson, M., "Blanket/First wall challenges and required R&D on the pathway to DEMO", Fusion Engineering and Design, 100:2-43 (2015).
[16] Brooks J.N., El-Guebaly L., Hassanein A. and Sizyuk T. (2015), Nucl. Fus. 55 043002
[17] Fabritsiev S.A., Gosudarenkova V.A., Potapova V.A., Rybin, V.V., Kosachev L.S., Chakin V.P., Pokrovsky A.S. and Barabash V.R. 1992 J. Nucl. Mater. 191–4 426–9
[18] Rieth M. et al 2013 J. Nucl. Mater. 432 482–500
[19] Ueda Y. et al 2017 Nucl. Fus. 57 092006
[20] Gilbert M.R., Packer L.W., Sublet J. and Forrest R.A. 2014, Nucl. Sci. Eng. 177 291–306.
[21] D.A. Pappas, B. Lipschultz, B. LaBombard, M.J. May, C.S. Pitcher, “Molybdenum sources and transport in the Alcator C-Mod tokamak”, Journal of Nuclear Materials, Volumes 266–269, (1999), Pages 635-641, ISSN 0022-3115, https://doi.org/10.1016/S0022-3115(98)00597-2.
[22] S. R. Breon, N. R. Chellew, R. G. Clemmer, and J. C. Hoh, "GAMMA IRRADIATION OF NITRATE-BASED SALTS", ANL/FPP/TM-129, (March 1980).
[23] Fernández, A.G., Galleguillos, H., Fuentealba, E. et al., "Thermal characterization of HITEC molten salt for energy storage in solar linear concentrated technology", J. Therm. Anal. Calorim. 122, 3–9 (2015), https://doi.org/10.1007/s10973-015-4715-9.
[24] Creely, A., Greenwald, M., Ballinger, S., Brunner, D., Canik, J., Doody, J., . . . Zhu, J. (2020). Overview of the SPARC tokamak. Journal of Plasma Physics, 86(5), 865860502. doi:10.1017/S0022377820001257
[25] https://www.fusionindustryassociation.org/fusion-energy-breakthrough-makes-global-headlines/
[26] National Academies of Sciences, Engineering, and Medicine. 2021. Bringing Fusion to the U.S. Grid. Washington, DC: The National Academies Press. https://doi.org/10.17226/25991.
[27] Masaru Nakamichi, Jae-Hwan Kim, Petr Kurinskiy, Characterization of vanadium beryllide pebble bed for the Japan DEMO blanket application, Fusion Engineering and Design, Volume 136, Part A, (2018), Pages 125-127, ISSN 0920-3796, https://doi.org/10.1016/j.fusengdes.2018.01.022.
[28] Rozenkevich, M.B., Kulov, N.N., Pak, Y.S. et al., Removal of Tritium from Gas Flows from Working Areas of Nuclear Facilities. Theor Found Chem Eng 57, 239–247 (2023). https://doi.org/10.1134/S0040579523030156
[29] Steven J. Zinkle, Jeremy T. Busby, Structural materials for fission & fusion energy, Materials Today, Volume 12, Issue 11, 2009, Pages 12-19, ISSN 1369-7021, https://doi.org/10.1016/S1369-7021(09)70294-9.

[30] J. S. Przybyszewski, FRICTION AND CONTACT RESISTANCE FOR LOW-SPEED GALLIUM-LUBRICATED SLIDING ELECTRICAL CONTACTS OF BERYLLIUM I N VACUUM, Lewis Research Center Cleveland, Ohio, NASA TN D-5706.
[31] J. Neubrand, C. Bilgen & H. Weiss (1995) Rolling wear of tin coatings induced by non-uniform hertzian stress distribution, Surface Engineering, 11:2, 133-137, DOI: 10.1179/sur.1995.11.2.133
[32] M.S. Tillack, University of California – San Diego (retired), presentation at the Fusion Blanket Technologies Virtual Workshop. Hosted by EPRI Charlotte, 4 May 2023.
[33] Kurt Kugeler, Zuoyi Zhang, "Modular High-temperature Gas-cooled Reactor Power Plant", Springer, January 2019 DOI:10.1007/978-3-662-57712-7 ISBN: 978-3-662-57710-3.
[34] Marchhart, T., Hargrove, C., Marin, A. et al. Discovering tungsten-based composites as plasma facing materials for future high-duty cycle nuclear fusion reactors. Sci Rep 14, 13864 (2024). https://doi.org/10.1038/s41598-024-64614-3
[35] A. Ying, M. Abdou, C. Wong, S. Malang, N. Morley, M. Sawan, B. Merrill, D.K. Sze, R. Kurtz, S. Willms, M. Ulrickson, S. Zinkle, "An overview of US ITER test blanket module program", Fusion Engineering and Design, Volume 81, Issues 1–7, (2006), Pages 433-441, ISSN 0920-3796, https://doi.org/10.1016/j.fusengdes.2005.06.379.
[36] Sabina Griffith, "First design review within Test Blanket Module Program", 9 Jul 2013, https://www.iter.org/node/20687/first-design-review-within-test-blanket-module-program
[37] "Europe ready to prove the fabrication of Test Blanket Modules", https://fusionforenergy.europa.eu/news/europe-ready-to-prove-the-fabrication-of-test-blanket-modules/
[38] "ITER Test Blanket System passes Conceptual Design Review", https://fusionforenergy.europa.eu/news/iter-test-blanket-system-passes-conceptual-design-review/
[39] C.E. Kessel, J.P. Blanchard, A. Davis, L. El-Guebaly, L.M. Garrison, N.M. Ghoniem, P.W. Humrickhouse, Y. Huang, Y. Katoh, A. Khodak, E.P. Marriott, S. Malang, N.B. Morley, G.H. Neilson, J. Rapp, M.E. Rensink, T.D. Rognlien, A.F. Rowcliffe, S. Smolentsev, L.L. Snead, M.S. Tillack, P. Titus, L.M. Waganer, G.M. Wallace, S.J. Wukitch, A. Ying, K. Young, Y. Zhai, "Overview of the fusion nuclear science facility, a credible break-in step on the path to fusion energy", Fusion Engineering and Design, Volume 135, Part B, (2018), Pages 236-270, ISSN 0920-3796, https://doi.org/10.1016/j.fusengdes.2017.05.081
[40] M. E. Rising, J. C. Armstrong, S. R. Bolding, F. B. Brown, J. S. Bull, T. P. Burke, A. R. Clark, D. A. Dixon, R. A. Forster III, J. F. Giron, T. S. Grieve, H. G. Hughes III, C. J. Josey, J. A. Kulesza, R. L. Martz, A. P. McCartney, G. W. McKinney, S. W. Mosher, E. J. Pearson, C. J. Solomon Jr., S. Swaminarayan, J. E. Sweezy, S. C. Wilson, A. J. Zukaitis. MCNP® Code Version 6.3.0 Release Notes. Los Alamos National Laboratory Tech. Rep. LA-UR-22-33103, Rev. 1. Los Alamos, NM, USA. January 2023.
[41] M. E. Rising, J. C. Armstrong, S. R. Bolding, F. B. Brown, J. S. Bull, T. P. Burke, A. R. Clark, D. A. Dixon, R. A. Forster III, J. F. Giron, T. S. Grieve, H. G. Hughes III, C. J. Josey, J. A. Kulesza, R. L. Martz, A. P. McCartney, G. W. McKinney, S. W. Mosher, E. J. Pearson, C. J. Solomon Jr., S. Swaminarayan, J. E. Sweezy, S. C. Wilson, A. J. Zukaitis. MCNP® Code Version 6.3.0 Release Notes. Los Alamos National Laboratory Tech. Rep. LA-UR-22-33103, Rev. 1. Los Alamos, NM, USA. January 2023.
[42] L. Zou, J.W. Peterson, R.C. Martineau, R.N. Slaybaugh, A. J. Novak, "Pronghorn: A Porous Media ThermalHydraulics Core Simulator and its Validation with the SANA Experiments", INL/CON-18-44290-Revision-0, April 2018.